ELSEVIER

Computers & Geosciences 32 (2006) 1205–1220

COMPUTERS & GEOSCIENCES

www.elsevier.com/locate/cageo

ModDRE: A program to model deepwater-reservoir elements using geomorphic and stratigraphic constraints ☆

Zulfiquar A. Reza*, Matthew J. Pranter, Paul Weimer

Energy and Minerals Applied Research Center, Department of Geological Sciences, UCB 399, University of Colorado, Boulder, CO 80309-0399, USA

Received 24 June 2005; received in revised form 12 November 2005; accepted 14 November 2005

Abstract

In deepwater-reservoir modeling, the proper representation of the spatial distribution of architectural elements is important to account for pore-volume distribution and the connectivity of reservoir sand bodies. This is especially critical for rock and fluid-volume estimates, reservoir-performance predictions, and development-well planning.

A new integrated stochastic reservoir-modeling approach (ModDRE—**Mod**eling **D**eepwater **R**eservoir **E**lements) accounts for geomorphic and stratigraphic controls to generate the deepwater-reservoir architecture. Information on stratal-package evolution and sediment provenance can be integrated into the reservoir-modeling process. A slope-area analytical approach is implemented to account for topographical constraints on channel and sheet-form reservoir architectures and their distribution. Inferred sediment–source statistics and architectural-element variability (from seismic, outcrop, and stratigraphic studies) associated with relative changes in sea level can also be used to constrain the deepwater-reservoir-element statistics. Based on these geomorphic and stratigraphic constraints, deepwater-reservoir elements (channels, lobes) are built into the model sequentially (in stratigraphic order).

Integration of realistic geological and engineering attributes into deepwater-reservoir models is vital for optimal reservoir management. This approach is unique in that it is more directly constrained to geomorphic and stratigraphic parameters than traditional object- or surface-based techniques for stochastic deepwater-reservoir modeling.

Keywords: Deepwater-reservoir modeling; Deepwater-reservoir architecture; Geomorphic parameterization; Stratigraphic controls; Stratigraphic–sedimentologic modeling

1. Introduction

Our understanding of the reservoir architecture of deepwater systems has improved with recent advances in imaging of the shallow and deep subsurface and through characterization with outcrop analogs. However, we do not have a complete knowledge of the subsurface environment, so a high degree of uncertainty remains when building deepwater-reservoir models. Stochastic modeling

☆ Executable of the source code available from http://emarc.colorado.edu/respubs/programs/dw_mod.html

*Corresponding author. Tel.: +1 303 492 2126; fax: +1 303 492 2606.

E-mail addresses: zulfiquar.reza@colorado.edu (Z.A. Reza), matthew.pranter@colorado.edu (M.J. Pranter), paul@emarc.colorado.edu (P. Weimer).

0098-3004/$ - see front matter © 2005 Elsevier Ltd. All rights reserved.
doi:10.1016/j.cageo.2005.11.004

approaches are useful because they provide a means of quantifying uncertainty through generation of multiple realizations of reservoir property models. A number of stochastic modeling techniques are presently available for building deepwater-reservoir models that can be broadly classified into three categories: (1) *cell-based* approaches that primarily implement two-point geostatistics (Deutsch and Journel, 1998), and more recently multipoint-geostatistical concepts (Strebelle et al., 2002); (2) o*bject-based* or *Boolean* approaches have been used to build more geologically realistic reservoir models that incorporate nonlinear features (Haldorsen and Lake, 1984; Haldorsen and Chang, 1986; Jones, 2001, and Deutsch and Tran, 2002). The geologic objects are conditioned to hard data (e.g. wells) and also honor stratigraphic relationships and interpretations; (3) *stochastic surface-based* techniques (Xie et al., 2000; Pyrcz et al., 2005) have been used to capture the compensational stacking tendency of flow-event deposits within deepwater lobes.

In contrast to stochastic methods, process-based methods attempt to simulate fundamental geological processes to produce a numerical representation of the reservoir geology (Tetzlaff and Harbaugh, 1989; Martinez and Harbaugh, 1993). Process-based approaches include the rigor of the physics of sedimentation and depositional processes. However, enormous difficulties arise when it comes to conditioning process-based models to existing data (e.g., honoring well and seismic data).

In this study, we introduce a novel approach to deepwater-reservoir modeling (called ModDRE—**Mod**eling **D**eepwater **R**eservoir **E**lements) that attempts to mimic the geologically realistic results of process-based techniques but incorporates stochasticity throughout the modeling process. This approach is implemented using Fortran. A combination of concepts is adopted in this approach to honor geomorphic and stratigraphic constraints. In this paper, we use various terms and nomenclature related to our approach. For clarification, brief explanations of many of the terms we use are presented in Table 1. To identify flow paths for deepwater channels and lobes, concepts from hypsometric analysis of channelized flow are incorporated. The spatial variability in deepwater architecture that is common within a sequence-stratigraphic framework is incorporated through inputs for initial bathymetry, sediment–source location, channel and lobe (sheet) dimensions, channel erosion/deposition, and other controls that can vary stratigraphically.

2. Methodology

ModDRE is a deepwater-reservoir-modeling approach that incorporates geomorphic and stratigraphic constraints. ModDRE simulates the deposition of deepwater channels, lobes (sheets), and condensed sections (or hemipelagic shale). The program simulates one channel and associated lobe at one time and constructs the deepwater stratigraphy starting at the base (initial bathymetric surface) of the model domain and builds upward through the model domain by adding successive channel-lobe deposits. Thus, the algorithm proceeds with an interpreted initial bathymetry (for example, from 3D seismic data) upon which deposition of the channels and lobes stack to produce the desired stratigraphic architecture. The bathymetry of an area is a function of the local and regional structure, stratigraphy, and other factors. Bathymetry is important because it affects sedimentation. In this approach, we assume that an interpretation of the initial bathymetric surface is complete. The ModDRE approach can be used to model multiple realizations of deepwater reservoirs using different interpretations of the initial bathymetric surface. The model domain could represent deposits within a confined intraslope minibasin, as well as an unconfined deepwater setting. The orientation, length, sinuousity, and dimensions of a channel are controlled by the initial and subsequent bathymetric surfaces and other constraints that are discussed.

The process of modeling deepwater-reservoir elements and architecture has several steps. We start with the geomorphic parameterization of the initial bathymetric surface (or as it exists in any arbitrary time). The goal is to compute several parameters that constrain placement of the reservoir-architectural elements. Then, the channel-entry point or starting grid cell of the channel into the basin is determined. After the channel-entry point is selected, our next steps attempt to answer the following questions through the modeling process: (1) where and how will the channels be placed? (2) how much erosion exists at the base of the channel? and (3) what are the geometries of the channel and channel-fill deposits? Once the channels and channel-fill deposits are modeled, similar modeling strategies are used for placing the deepwater

Table 1
Descriptions of terms

Term	Description
Reservoir element	A part of a reservoir characterized by unique stratigraphic and petrophysical properties that distinguishes it from other parts of a reservoir (e.g., channel or lobe).
Reservoir architecture	Spatial arrangement and geometry of reservoir elements (e.g., lateral continuity and stacking of sedimentary deposits).
Stratigraphic	Refers to nature and characteristics of various parameters (e.g., channel thickness, channel aspect ratio, channel erosion, channel-fill thickness).
Geomorphic	In this paper, geomorphic refers to bathymetry and parameters derived from bathymetry. These include sediment-flow vector (slope, azimuth), contributing area, and erodability index.
Bathymetry	z-value (water depth) at a grid cell in model domain.
Channel	Elongate negative-relief features produced and/or maintained by turbidity/current flow.
Channel fill	Sediments that were deposited within [channel] depression.
Sheet	Sheet sands and sandstones have lobate forms at termini of channels. They reflect sediments that have bypassed through updip channels [confined flow] and are characterized by high-aspect-ratio reservoir sand bodies (>500:1).
Lobe	Areas of sand deposition in modern systems lie immediately downslope from main channel. Although not specifically modeled in our current approach, lobes can consist of layered or amalgamated sheets with excellent continuity.
Sediment-flow vector	Vector representation of likely flow-path of sediments. It has a slope and direction (azimuth) associated with it and is computed from bathymetry.
Slope	A grid-cell value of slope of sediment-flow vector, in radians/degrees.
Angle	A grid-cell value of azimuth of sediment-flow vector, in radians/degrees.
Pointer	A grid-cell value to reference one of its eight adjacent cells.
Contributing area	A grid-cell value that corresponds to amount of upslope area likely to contribute to sediment transport to that cell.
Erodability index	A grid-cell value corresponding to likelihood of erosion in that cell based on slope and contributing area. A high erodability index corresponds to high slope and/or contributing area.
Channel trajectory	Computed course (path) of a deepwater channel.
Distributary branches	Branches are used solely as a modeling method to create a deepwater lobe form. Near end of channel trajectory, distributary branches extend outward in various directions and with various lengths to produce a range of deepwater lobe geometries.
Net-to-gross ratio	Proportion of net-sand thickness to overall thickness at a grid cell in model domain.

lobes (sheets). Finally, a thin hemipelagic shale interval or condensed section can be modeled based on the concept of pelagic or hemipelagic sedimentation in deepwater settings. A detailed description of each of these steps follows.

2.1. Geomorphic parameterization

The geometry and distribution of deepwater channels, channel fills, and lobes (sheets) vary considerably in response to changes in gradient of the bathymetric surface, so characteristics of the bathymetry must be considered. Several geomorphic parameters are evaluated using the initial and subsequent post-depositional bathymetric surfaces. Of these, the sediment-flow vector and contributing area (Table 1) of each grid cell are computed first (Figs. 1 and 2). We define the sediment-flow vector as the vector representation of the likely direction of sediment flow. The contributing area refers to the value assigned to a grid cell that represents the amount of upslope area that can contribute to sediment transport to that cell (all upslope cells that can contribute; not only adjacent upslope cells).

First consider the sediment-flow vector. We use a modified version of the D_∞ multiple flow-direction model as presented by Tarboton (1997) to calculate sediment-flow vectors across the initially interpreted and subsequently computed bathymetric surfaces (Fig. 1). This procedure represents flow direction as a vector in the direction of the steepest downward slope on eight triangular facets centered at each grid cell (Fig. 1). An infinite number of flow directions are possible having angles between 0° and 360° (thus the symbol D_∞). The two downslope grid cells closest to the vector flow-angle share the flow from a grid cell on the basis of angle proportioning as indicated in Fig. 1C.

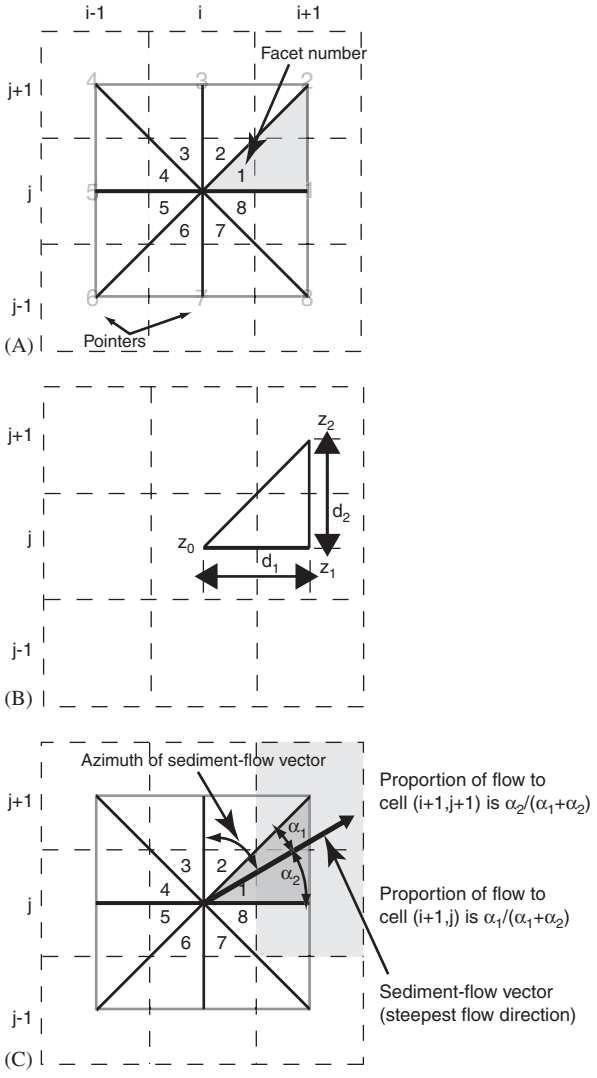

Fig. 1. Schematic diagram to illustrate several components to compute sediment-flow vector as part of geomorphic parameterization. (A) Relationship between global grid cell and local facet indexing in sediment-flow-vector computation. Table 2 lists projections from global to local indices (and visa versa). (B) Bathymetry and distance variables to compute slope and angle for one facet (in this case, facet 1). (C) Illustration to show proportioning of flow to adjacent grid cells. Two cells $[(i+1, j+1)$ and $(i+1, j)]$ that are highlighted in gray will receive sediment flow from central grid cell (i, j). Modified from Tarboton (1997).

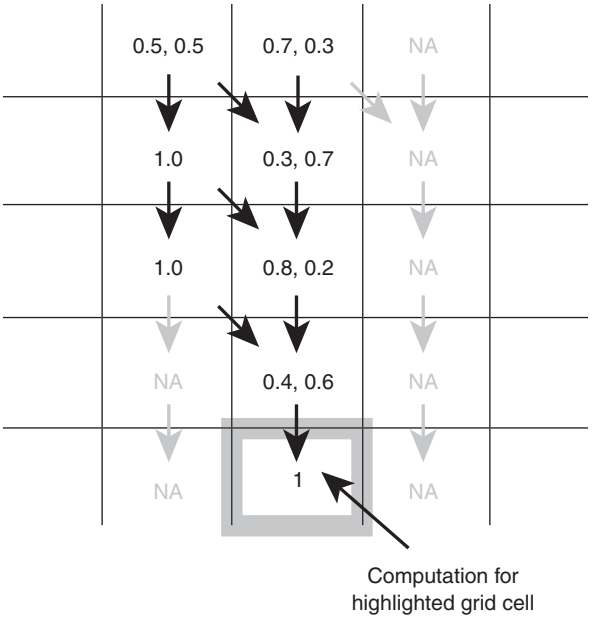

Fig. 2. Schematic diagram to illustrate computation of contributing area as part of geomorphic parameterization. This contributing area is calculated for cell highlighted by bold gray rectangle. Numbers in each grid cell correspond to proportion of flow coming from adjacent upslope grid cell(s). Arrows show sediment-flow-vector directions. Black arrows correspond to grid cells that contribute sediment flow to highlighted grid cell (i.e., they are part of upslope area for highlighted grid cell). Gray arrows correspond to grid cells that do not contribute sediment flow to highlighted grid cell. NA = not applicable.

Calculation of the sediment-flow vector is as follows (modified from Tarboton, 1997). For all grid cells, pointers 1–8 are assigned to adjacent cells for referencing (Fig. 1A). Pointers are used during the modeling process for various referencing reasons. Eight triangular facets exist between a grid cell and its eight adjacent cells in a 3×3 grid-cell window (Fig. 1A). Each of these facets has one downslope vector with the maximum angle of descent. The outward projection of this downslope vector from the center of the grid cell will lie within or outside the facet of interest. If the downslope vector lies outside the facet, then the angle between the vector and the adjacent facet margin cannot exceed 45°, and the sediment-flow direction for that facet is assigned the direction of the adjacent facet edge. The sediment-flow vector assigned to the grid cell is the steepest of the downslope vectors among the eight facets. For a single triangular facet (Fig. 1B), downward slope is represented by the vector (s_1, s_2) where

$$s_1 = (z_0 - z_1)/d_1, \tag{1}$$

$$s_2 = (z_1 - z_2)/d_2, \tag{2}$$

where z_i and d_i are bathymetry and distance values between grid cells indicated in Fig. 1. The slope

direction and magnitude are computed using

$$r = \tan^{-1}(s_2/s_1), \quad s = \sqrt{s_1^2 + s_2^2}. \tag{3}$$

If r is not in the range $(0, \tan^{-1}(d_2/d_1))$ then r is set as the direction along the appropriate edge and s assigned as the slope along that edge, as

$$\text{if } r<0, \quad \text{set } r = 0, \quad s = s_1,$$
$$\text{if } r>\tan^{-1}(d_2/d_1), \quad \text{set } r = \tan^{-1}(d_2/d_1),$$
$$s = (z_0 - z_1) \Big/ \sqrt{d_1^2 + d_2^2}. \tag{4}$$

Mapping of any facet bathymetry and distance values to corresponding values on the eight-facet system (Fig. 1) is arranged such that z_0 is the center point, z_1 is the lateral point, and z_2 is the diagonal point of each facet. The local angle corresponding to the largest downward slope of the eight facets ($r' = r$ with maximum s) is converted to azimuth to obtain the sediment-flow direction using the following equation:

$$r_g = \alpha_f r' + \alpha_c \pi/2, \tag{5}$$

where α_f and α_c are defined in Table 2 for the eight facets. Table 2 values differ from Tarboton (1997) because of the definition of the azimuth and coordinate orientation adopted in this work.

The goal of using contributing area in this modeling approach is that it identifies the likelihood that sedimentation could take place at a cell based on the amount of the upslope area that could contribute sediment to that cell location. The greater the contributing area of a grid cell, the more likely that depositional events will occur in that cell. To compute contributing area for a cell, all upslope cells that contribute to deposition to the cell are included. Thus, the contributing area to each grid cell, $a(i,j)$, is evaluated by (modified from Tarboton, 2003)

$$a(i,j) = \Delta + \sum_{k \text{ contributing adjacent cells}} p_k a(i_k, j_k), \tag{6}$$

where p_k is the proportion of flow from the adjacent grid cell k that contributes to the grid cell (i,j); Δ is area of each grid cell. Note that Eq. (6) is a recursive equation; all upstream cells are considered. The proportion of flow, p_k, for each adjacent grid cell is determined as indicated in Fig. 1C. An example of the contributing-area calculation is provided in Fig. 2.

Table 2
Global grid-cell and local facet-indexing for local to global mapping of parameters in sediment-flow-vector computation (modified from Tarboton, 1997)

Facet	Z_0	Z_1	z_2	α_c	α_f
1	$z_{i,j}$	$z_{i+1,j}$	$z_{i+1,j+1}$	1	−1
2	$z_{i,j}$	$z_{i,j+1}$	$z_{i+1,j+1}$	0	1
3	$z_{i,j}$	$z_{i,j+1}$	$z_{i-1,j+1}$	4	−1
4	$z_{i,j}$	$z_{i-1,j}$	$z_{i-1,j+1}$	3	1
5	$z_{i,j}$	$z_{i-1,j}$	$z_{i-1,j-1}$	3	−1
6	$z_{i,j}$	$z_{i-1,j-1}$	$z_{i-1,j-1}$	2	1
7	$z_{i,j}$	$z_{i-1,j-1}$	$z_{i+1,j-1}$	2	−1
8	$z_{i,j}$	$z_{i+1,j}$	$z_{i+1,j-1}$	1	1

2.2. Channel-entry point

During the modeling process, deepwater channel and lobe reservoir elements are modeled with each channel beginning on the edge of the model domain. The entry point for a channel (channel-entry point) on the margin of the model domain is determined stochastically from a histogram of channel-entry-point azimuths that indicate the possible points from which a channel originates. Several rules are honored during the selection of a channel-entry-point location. The channel-entry point from which a channel reservoir-element originates is determined by, first, randomly selecting the azimuth for the proposed location from an input histogram (Fig. 3). The azimuth is determined from an origin in the center of the model domain (e.g., an azimuth of 90° indicates that the channel will originate on the

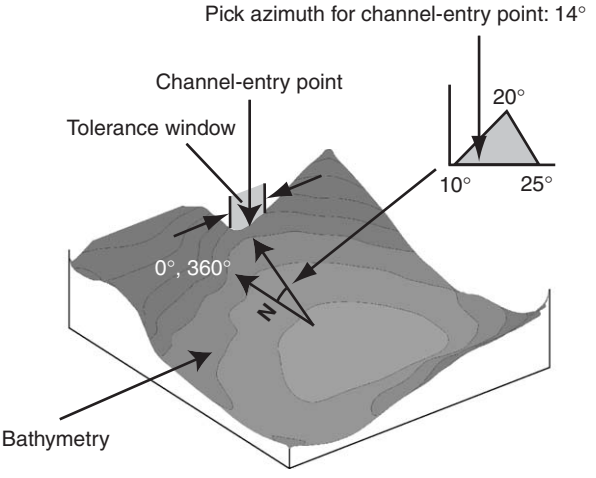

Fig. 3. Schematic diagram that illustrates selection of channel-entry point. Channel-entry point from which a channel reservoir element originates is determined by, first, randomly selecting azimuth for proposed location from an input histogram. Final channel-entry-point location is selected from within a tolerance window surrounding proposed location for channel-entry point.

model's edge from due east). The final channel-entry-point location is selected from within a tolerance window surrounding the proposed location for the channel-entry point. Within the tolerance window, pointers (calculated previously in geomorphic parameterization) for all the grid cells are checked as to whether the downward slope direction points into the model domain. For all grid cells that have downward slope directions into the model domain, the grid cell with the lowest elevation is picked as the starting point (channel-entry point) of the channel trajectory.

2.3. Sequence-stratigraphic controls

A number of sequence-stratigraphic controls are integrated into the modeling approach. The architectural elements that are modeled include single-story channels (that can stack into channel complexes), accompanying deepwater lobes (sheets), and condensed sections. The channels can be erosional, depositional, or a combination of both erosional and depositional (Weimer and Slatt, 2004). Updip-to-downdip aspect ratios (width-to-thickness ratios) of the channel fill a range from as low as 10:1 to approximately 50:1. Channel width increases downdip for all channels.

Channel erosion occurs along the length of the channel and stops when the channel trajectory encounters a mean gradient value that is less than a specified threshold (e.g., 1.0°). The threshold value can vary depending on geological information of the sea floor, substrate, and depositional processes of a particular area. Where channel erosion ends, the channel becomes depositional in nature. Channel erosion is the maximum at the updip location. Erosion decreases basinward to zero at the erosion termination point in the channel. Erosion generally decreases across the channel width at any point along a channel trajectory. However, the amount of erosion across the channel width also depends on the local bathymetry. The channel-fill thickness is the same as the erosion thickness at the updip location and decreases downdip. Presently, the ModDRE approach does not model levees as distinct reservoir elements. Channel-fill thickness decreases across the channel width. The aspect ratio of the deepwater lobes (>500:1) is an order of magnitude greater than that of the channel bodies. Condensed-section thickness is an order of magnitude less than the updip channel-fill thickness. Variability in the initial (updip) channel thickness, channel aspect ratio, and channel-entry-point location is honored in the models from one channel-lobe depositional event to another based on the input histograms for these parameters (Fig. 4).

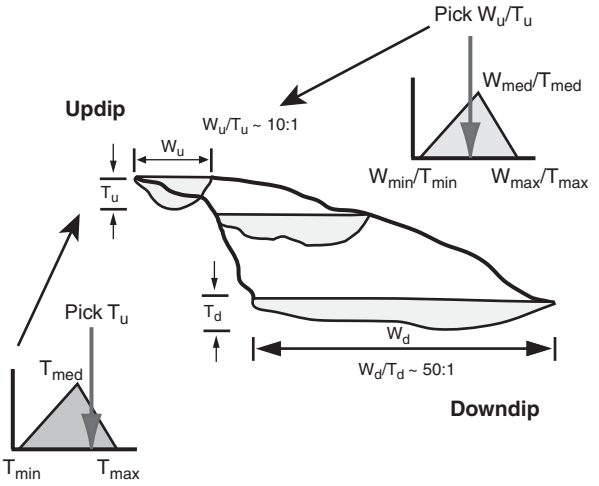

Fig. 4. Schematic diagram that illustrates selection of starting channel thickness and aspect ratio. These initial values are randomly selected from corresponding input triangular histograms. Updip-to-downdip aspect ratios (width-to-thickness ratios) of channel fill a range from as low as 10:1 to approximately 50:1. Channel width increases downdip for all channels. Channel-fill thickness decreases across channel width.

2.4. Channel-trajectory determination

Deepwater channels are defined as elongate, negative-relief features produced and/or maintained by turbidity current flow (Mutti and Normark, 1991). Channels represent relatively long-term pathways for sediment transport. Channel shape and position within a turbidite system are controlled by depositional processes and erosional downcutting or a combination of both processes (Mutti and Normark, 1991; Weimer and Slatt, 2004).

The location of a deepwater channel (herein referred to as channel trajectory) in the model domain is determined following several rules. The channel trajectory starts from the channel-entry-point location identified previously (Fig. 3). The channel trajectory is then computed for one grid cell at a time and generally in a basinward direction. For each cell along the presently computed channel trajectory, several parameters are computed that can influence the subsequent channel trajectory. These parameters include the tortuosity and curvature of the computed channel trajectory, local slope,

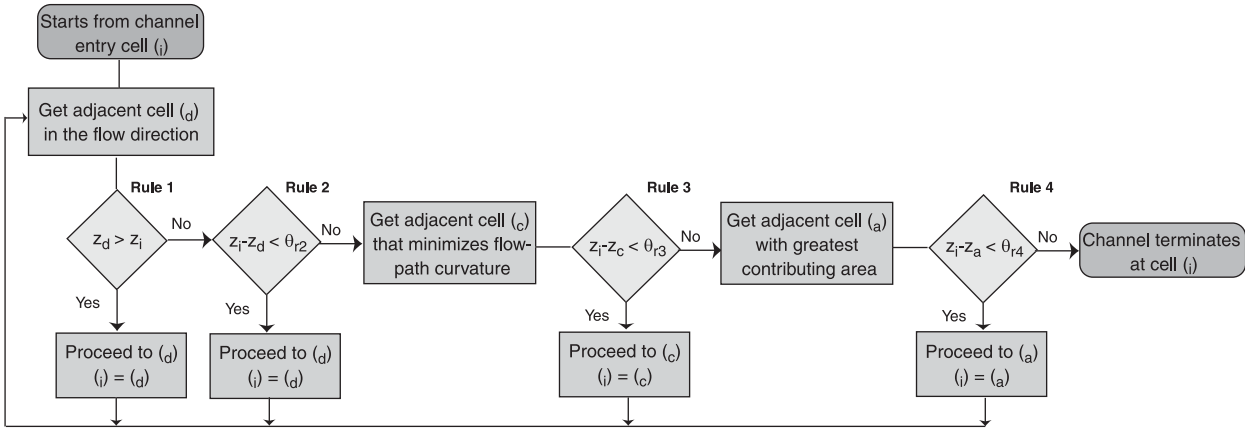

Fig. 5. Flow diagram to illustrate determination of channel trajectory. Trajectory starts at channel-entry point. Four rules (1–4) are depicted in a flow-chart that dictate how channel trajectory progresses. Variable z is bathymetry and θ is bathymetric threshold. Subscripts i, d, c, and a for variable z denote bathymetry values for initial or current grid cell, adjacent downslope cell, adjacent cell based on curvature rule, and adjacent cell based on contributing area rule, respectively. Subscripts r2, r3 and r4 for variable θ denote threshold values used in Rules 2, 3, and 4, respectively (see text for explanation).

mean (regional) slope, total bathymetric increase, and instantaneous bathymetric increase. To determine the channel trajectory, adjacent cells that would result in high values of tortuosity and/or curvature of the channel trajectory are excluded. The four main rules for channel trajectory determination are illustrated in a flow diagram (Fig. 5).

For each grid cell along the channel trajectory, the channel trajectory is directed from the current grid cell toward the cell in the direction of the steepest downward slope (Rule 1, Fig. 5). If, however, the current grid cell of the channel trajectory is deeper than the adjacent grid cells, the channel can still progress if the bathymetric difference between the deepest adjacent grid cell and the current grid cell is less than a threshold value (e.g., equivalent to 10% of the starting channel thickness) (Rule 2). A low threshold reflects a relatively low erosive energy of a deepwater sediment flow. If this rule is not met, then the channel trajectory can still progress to the adjacent grid cell that results in the minimum curvature for the channel trajectory (Fig. 5). The minimum curvature rule (Rule 3) will apply only if the bathymetric difference between the adjacent grid cell and the current grid cell is less than another threshold value (e.g., equivalent to 20% of the starting channel thickness). One point to note is that Rule 3 applies only when the first three rules fail, and thus this approach does not minimize the tortuosity and/or curvature of the channel trajectory in general. Our modeling experience with the developed approach is that Rule 3 is seldom encountered. If Rule 3 is not met, then the trajectory can progress to the adjacent cell with the greatest contributing area, if the bathymetric difference between the adjacent grid cell and the current grid cell is less than a greater threshold value than those used in Rules 2 and 3 (e.g., equivalent to 25% of the starting channel thickness) (Rule 4).

Along the channel trajectory, the threshold values used in the channel trajectory algorithm decrease basinward. These rules are used to approximate the erosive energy of the deepwater system. The threshold values decrease basinward to reflect the lower erosive energy of the system. Thus, it becomes more difficult for the channel to progress farther. The channel trajectory terminates when none of the criteria discussed above are encountered.

An important point to note about this modeling approach is that both local and regional information are used in the channel-trajectory determination. Sediment-flow vector, local slopes, instantaneous bathymetric variation, and other local parameters have strong influence on the channel trajectory. However, large-scale features like mean slope, total bathymetric increase, curvature and tortuosity also influence the channel trajectory.

2.5. Channel geometry

The geometries of open and filled channels change in response to changes in gradient, from a

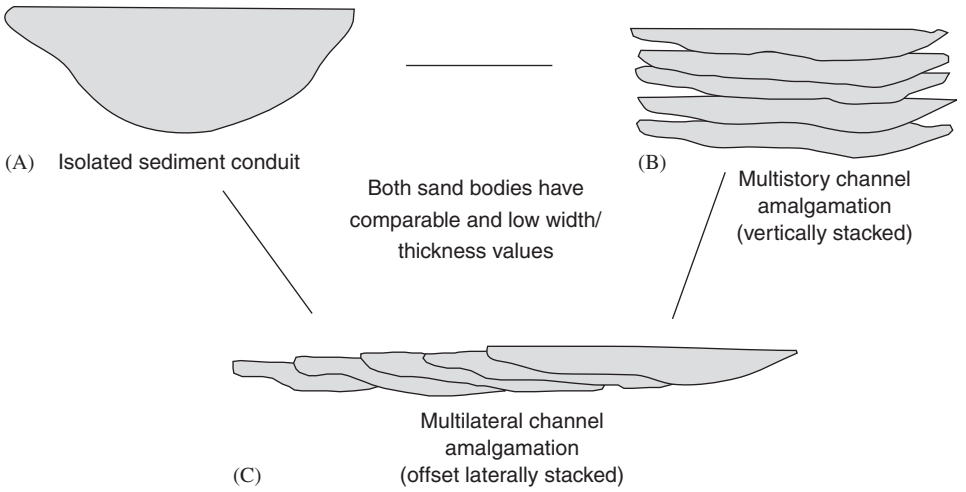

Fig. 6. Generalized variations in channel forms. (A) An erosional channel which may be deep and relatively low aspect ratio. (B) In a confined setting, such as a salt minibasin, channels may stack vertically (i.e., may be multistory). (C) In a less confined setting channels tend to migrate laterally, giving rise to multilateral amalgamation and a higher aspect ratio for entire deposit. Modified from Clark and Pickering (1996).

single deep feeder channel to shallower and broader channels and sets of channels in a more unconfined setting (Fig. 6; Weimer and Slatt, 2004). The width and the thickness of the channel along its trajectory are determined using the starting thickness and aspect-ratio values, θ_0 and α_0, respectively. These starting thickness and aspect-ratio values are randomly drawn from corresponding input histograms. The steps used in the calculation of width and thickness are as follows:

Starting width, w_0, is determined from

$$w_0 = \theta_0 \alpha_0. \tag{7}$$

Downdip aspect ratio, α_n, is determined using

$$\alpha_n = \alpha_0 A_\alpha, \tag{8}$$

where A_α is the aspect ratio increase factor, and n is the number of grid cells in the channel trajectory.

Downdip width, w_n, is determined using

$$w_n = w_0 A_w, \tag{9}$$

where A_w is width increase factor.

Downdip thickness, θ_n, is determined using

$$\theta_n = \theta_0 A_\theta, \tag{10}$$

where A_θ is thickness decrease factor. The factors used in Eqs. (8)–(10) are not independent of each other. They are related using

$$A_\theta = A_\alpha / A_w, \tag{11}$$

where only A_α and A_w are supplied, and A_θ is determined from Eq. (11).

For any grid cell, i, along the channel trajectory, the current aspect ratio is determined by

$$\alpha_i = \alpha_n - \frac{n-i+1}{n}(\alpha_n - \alpha_0), \quad i = 1, \ldots, n. \tag{12}$$

For any grid cell, i, along the channel trajectory, the current channel thickness is determined by

$$\theta_i = \theta_0 - \frac{i-1}{n}(\theta_0 - \theta_n), \quad i = 1, \ldots, n \tag{13}$$

and the current width is determined by

$$w_i = \theta_i \alpha_i, \quad i = 1, \ldots, n. \tag{14}$$

The end of erosion, n_s, is determined based on a specified mean-slope criterion during the channel-trajectory determination. The scour amount, $(\theta_s)_i$, of the current grid cell along the channel trajectory up to the scour-termination point is determined by

$$(\theta_s)_i = \left(1 - \frac{i-1}{n_s}\right)\theta_i, \quad i = 1, \ldots, n. \tag{15}$$

A similar approach is also utilized for lobe-distributary thickness and width. However, the aspect ratio of lobe-form bodies is maintained as an order of magnitude greater than that of the channel-form bodies. Also, for lobe-form bodies, no scour event is simulated.

2.6. Deepwater-lobe placement

Sheet sands are deposited from decelerating flows at the termini of channels to form deepwater lobes.

Sheet sands and sandstones and deepwater lobes reflect the sediments that have bypassed through updip channels (confined flow) and are deposited in a primarily unconfined setting. They are characterized by high-aspect-ratio reservoir sand bodies (>500:1), which differ markedly in aspect from the updip channels that feed them.

The placement of deepwater lobes is determined using the following approach. The deepwater lobes are modeled at the end of the channel trajectory using several distributary branches. The distributary branches are used solely as a modeling method to create a deepwater-lobe form and are not additional reservoir elements in the model. The distributary branches extend outward in various directions and with various lengths to produce a range of deepwater-lobe geometries. To create a lobe form, along the channel trajectory and near the end of the channel, a number of grid cells are identified based on gradient criteria. These grid cells are starting points for the distributary branches. The grid cells are selected where the local and mean gradients of the channel trajectory are less than some threshold values. Similar to the approach to determine the channel trajectory, these distributary branches are systematically advanced into the model, and these trajectories should not intersect with the channel trajectory from which they originate. The lobe form thickness randomly decreases outward from the distributary branches.

After channel-lobe deposition, hemipelagic shale or condensed section deposition can be simulated, when appropriate. The thickness of the hemipelagic shale or condensed section is, however, only a fraction of the thickness of the initial channel. Depending on the deepwater system, deposition of the condensed sections can be modeled following deposition of each channel-lobe feature or following several stacked channel-lobe events. A varying degree of stochasticity is incorporated wherever deemed suitable to simulate the randomness in the modeling approach.

3. Implementation issues

A Fortran program is written to implement this deepwater-reservoir modeling approach. There are two major data structures maintained in the program: (1) a local data structure for the current bathymetry (as it exists at any arbitrary time) for the channel, lobe, and condensed-section placement as detailed in previous sections; and (2) a global data structure for stacking and updating the model as it is being built successively. The local data structure comprises several 2D arrays. The 2D arrays include those for initial bathymetry, bathymetry after channel erosion, bathymetry after channel-lobe deposition, bathymetry after condensed-section deposition, sediment-flow-vector azimuth, sediment-flow-vector slope, sediment-flow-vector pointers, contributing area, and reservoir-element identifiers. Once the modeling of a single channel-lobe and condensed-section event is completed, three bathymetric surfaces (top surface of condensed section, top surface of channel-lobe surface, and post-channel-erosion surface) and reservoir element identifiers are stored in separate 2D arrays of the global data structure. The same local data structure is used for the subsequent depositional events.

After modeling a specified number of depositional events (n_e as specified in the input section discussed later), a final 3D array defining the model is constructed from top to bottom. The reason for the top-to-bottom approach is the fact that younger events may erode older surfaces. The final 3D geometry data are stored in the corner-point-geometry format. Horizontal positions of the cells are thus fixed; however, the vertical (bathymetric) z values will vary depending on the modeling of the depositional events. The vertical thickness of a grid cell can be as small as zero corresponding to no deposition in the cell. The storage requirement within the program may seem redundant, but it allows great flexibility in the program such as high vertical resolution of the models and stratigraphic ordering. An important issue to note is that the developed modeling approach does not use net-to-gross ratio as a stopping rule in the modeling. The specified number of depositional events is used as the stopping criteria.

4. Input data

The important input data used in the modeling are summarized in Table 3. Horizontal model dimension is determined by n_x and n_y (number of grid cells) and grid size d_x and d_y in X and Y directions, respectively. Any unit system can be used, however, consistency of the unit system should be maintained. The initial bathymetry data have X, Y and Z values in a bathymetry data file in GEOEAS/GSLIB format. There should be $n_x \times n_y$ data in the bathymetry data file. The number of

Table 3
Main inputs used in deepwater-reservoir-modeling approach

Inputs	Symbol/description
Model dimension	n_x and n_y in X and Y directions
Grid size	d_x and d_y in X and Y directions
Initial bathymetry	X, Y and Z values
Number of depositional events	n_e
Random-number seed	Rand_seed
Probability threshold	p $(0<p<1)$
Azimuths for channel-entry point	Azimuth angle
Starting channel thickness	θ_0
Starting channel aspect ratio	α_0
Channel aspect-ratio increase factor	A_α
Channel width increase factor	A_w

Table 4
Outputs generated from deepwater-reservoir-modeling approach

Outputs	Description
3D model of surfaces	In corner-point geometry format
Cell-activation number	1 = active, 0 = inactive
Reservoir-element model	Channel = 1, Lobe = 2, Shale = 0
Sediment-flow vector (azimuth and slope)	In GEOEAS/GSLIB format
Sediment-flow-vector pointer	In GEOEAS/GSLIB format
Post-erosion, post-depositional, post-condensed-section depositional surfaces	In GEOEAS/GSLIB format
Reservoir-element identifiers	In GEOEAS/GSLIB format
Contributing area	In GEOEAS/GSLIB format

depositional events (n_e) to be modeled is specified. A random number seed is input for introducing a varying degree of stochasticity. A probability-threshold value is specified between 0 and 1 and is used in the channel-trajectory-determination algorithm. Channel-entry point (azimuth) data are specified for identifying source location position for each channel-lobe depositional event. Three values of azimuth (minimum, mode and maximum) are given for each depositional event. This specifies the triangular distribution from which one azimuth value is randomly drawn. Starting thickness and starting width-to-thickness aspect ratio for each channel-lobe depositional event are specified. Similar to source-direction data, triangular distributions specifications are input. Downdip-channel aspect-ratio increase factor and channel-width increase factor are also specified. In this approach, we have incorporated user specifications for each individual channel. We believe this allows greater flexibility in the modeling process. Variation due to eustacy or other appropriate influences can be accounted for in the specifications for individual channels. When this information is lacking, as in many cases, the modeler can use general information of the channel parameters and input identical specifications for all the channels.

5. Output

The outputs from ModDRE are presented in Table 4. A 3D model of the channel-lobe, and condensed-section deposits is generated in corner-point-geometry (ECLIPSE format, ECLIPSE, 2004) format. Active cells in the reservoir as used in ECLIPSE are output. Facies identifiers are output (Shale—0, Channel—1, and Lobe—2) in ECLIPSE property-file format. For initial bathymetry and after each channel-lobe, and condensed section depositional event, a number of parameters are generated particularly for debugging and critical analysis. These parameters include sediment-flow vector and pointer, post-erosion, post-deposition, post-condensed-section bathymetry, reservoir-element identifiers, and contributing areas. All of these are generated in a unified file in GEOEAS/GSLIB format. The 3D model files can be easily used in 3D visualization or reservoir-simulation packages.

6. Modeling example

We present an application of ModDRE for deepwater-reservoir modeling. A $6.5 \times 6.0\,km^2$ area is gridded into 650×600 areal grid cells. Each cell dimension is $10\,m \times 10\,m$. The initial bathymetry is shown in Fig. 7A. In this example, there is a basin in the middle portion of the area that could represent an intraslope basin. We modeled 14 channel-lobe and condensed-section events in this example. The variations in azimuths for channel-entry points, updip channel thickness, and width-to-thickness aspect ratio for all events are shown in Tables 5, 6 and7, respectively. The numbers in the tables define the minimum, mode, and maximum values of the triangular input histograms. Values for the parameters are randomly drawn from the triangular histograms. For every event, updip-to-downdip width and width-to-thickness aspect-ratio increment factors are 2.5 and 3.0, respectively. Along a channel trajectory, where the gradient reaches a

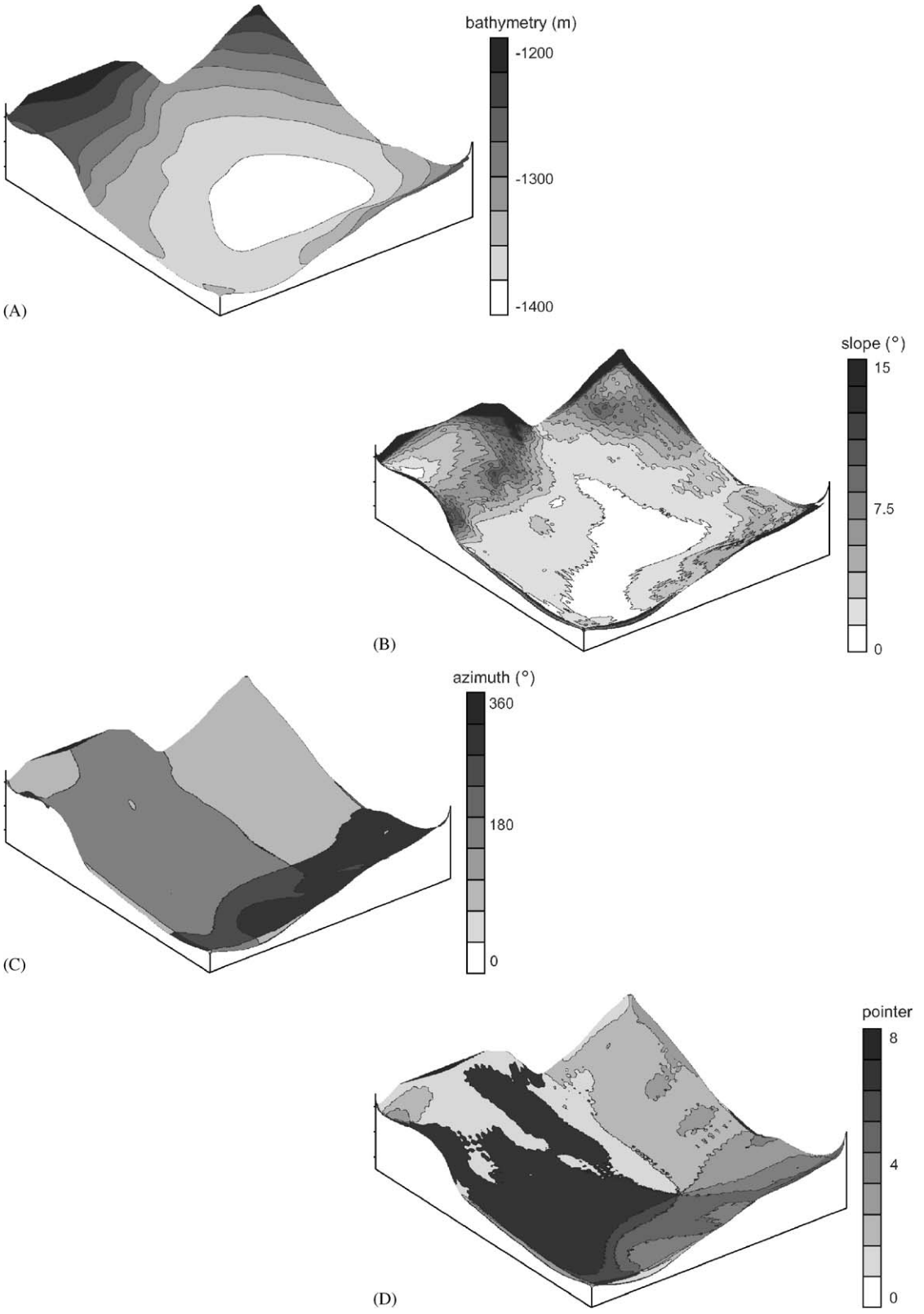

Fig. 7. Maps of (A) initial bathymetry, (B) slope of sediment-flow vector, (C) angle of sediment-flow vector, and (D) pointer for simple example discussed.

Table 5
Input variation in channel-entry-point azimuth in a triangular distribution form (minimum, mode and maximum define triangular distribution)

Event	Channel-entry point (radian)		
	Minimum	Mode	Maximum
1	5.00	5.02	5.05
2	4.96	4.97	4.99
3	5.04	5.06	5.10
4	4.97	5.01	5.04
5	5.06	5.09	5.13
6	4.93	4.95	4.97
7	5.09	5.12	5.15
8	5.02	5.05	5.07
9	4.96	4.97	4.99
10	4.93	4.95	4.97
11	5.05	5.07	5.11
12	4.97	5.01	5.04
13	4.92	4.94	4.96
14	5.02	5.05	5.08

Table 6
Input variation in starting channel thickness in a triangular distribution form (minimum, mode and maximum define triangular distribution)

System	Starting channel thickness (m)		
	Minimum	Mode	Maximum
1	9.15	10.20	11.25
2	9.65	9.70	10.75
3	9.15	11.20	12.25
4	10.15	11.20	12.25
5	11.25	12.30	14.35
6	10.15	12.20	13.25
7	9.15	10.20	11.25
8	8.15	9.20	10.25
9	8.15	9.20	10.25
10	9.15	10.20	11.25
11	10.15	12.20	13.25
12	11.15	11.20	12.25
13	10.15	10.20	10.25
14	11.15	11.20	11.25

Table 7
Input variation in starting channel width-to-thickness aspect ratio in a triangular form (minimum, mode and maximum define triangular distribution)

System	Starting channel width-to-thickness aspect ratio		
	Minimum	Mode	Maximum
1	8.15	9.20	10.25
2	9.65	10.70	11.75
3	10.15	11.20	12.25
4	11.15	12.20	13.25
5	10.25	11.30	12.35
6	9.15	10.20	11.25
7	8.15	9.20	10.25
8	9.15	10.20	11.25
9	10.15	11.20	12.25
10	9.65	10.70	11.75
11	10.15	10.20	10.25
12	11.15	11.20	11.25
13	10.25	10.30	10.35
14	10.15	10.20	10.25

value of 1.75°, erosion terminates and the channel becomes completely depositional. For the initial surface, the sediment-flow vector slope and azimuth and the corresponding pointer (Table 1) maps are shown in Fig. 7.

Fig. 8 illustrates the 3D model for all 14 modeled events. Three cross-sections (AA′, BB′, and CC′) show the proximal, intermediate, and distal stacking patterns of the channel-lobe and condensed-section events. The proximal cross-section, AA′ (Fig. 9), clearly shows compensational channel stacking and the erosion surfaces. The net-to-gross ratio is highest in this intersection. The intermediate cross-section, BB′, reveals a lower degree of erosion/scour and lower net-to-gross ratio. The degree of confinement decreases at this location compared to the proximal location. The distal cross-section, CC′, shows the sheet-form nature of the reservoir architecture. Also evident is the lower net-to-gross ratio in the distal region. A longitudinal cross-section, DD′, illustrates the continuity patterns of the architecture. A high degree of discontinuity is evident in the updip region due to channel erosion and sinuosity (Fig. 9, left side of DD′). Continuity increases in the downdip region particularly with the deposition of wider channels and sheet-form lobes. The updip-to-downdip thickness decrease is also evident in this longitudinal intersection. The modeled architectural features are also in agreement with conceptual geological views of the deepwater-reservoir architectures (Beaubouef et al., 1999, 2003; Johnson et al., 2001).

Importantly, ModDRE attempts to mimic the conceptual depositional and erosional processes in deepwater settings unlike purely stochastic approaches. Through this modeling process, realistic deepwater-reservoir architectures are produced. The

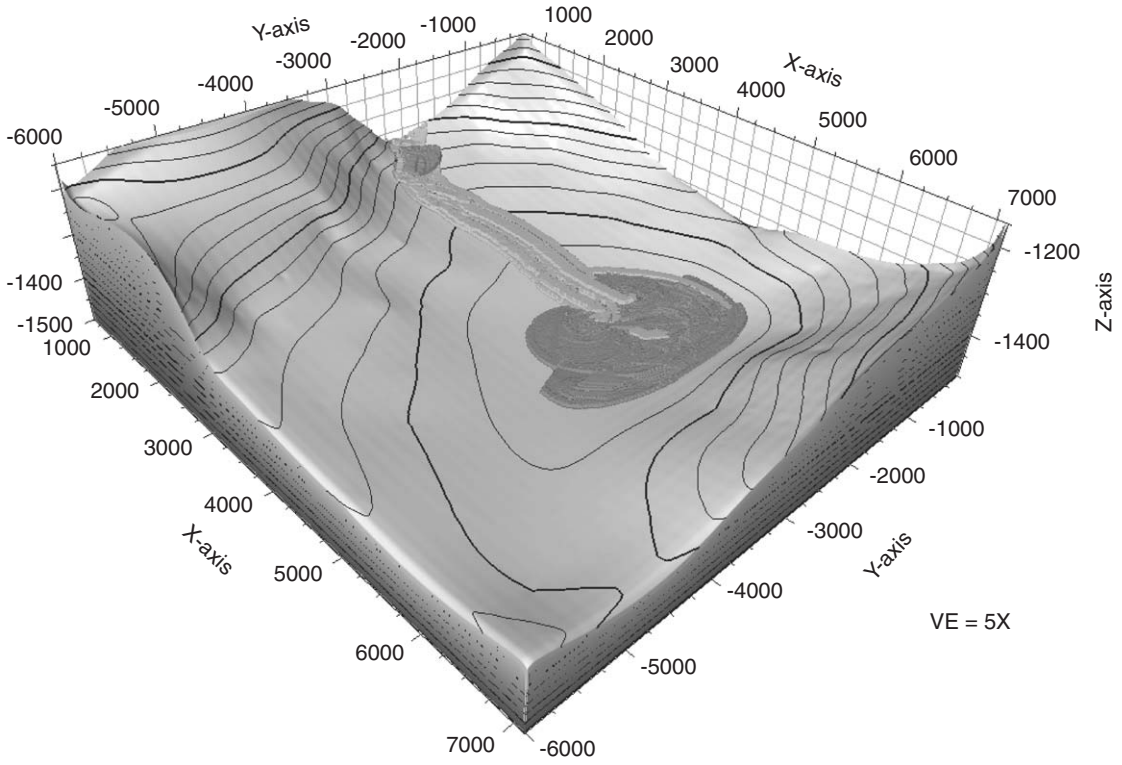

Fig. 8. 3D view of 14 channel-lobe events modeled in simple example discussed.

motivation for this approach was to incorporate both stratigraphic and geomorphic information, conceptual and quantitative. Through this modeling approach, it is possible to quantify the tortuosity, curvature, gradients, bathymetric change, and a number of other parameters for channel bodies and corroborate those with our understanding of these systems. It is also possible to control these parameters in the modeling approach. An important advantage of this approach is that it is computationally efficient. For the modeling example demonstrated above (grid cells $650 \times 600 \times 28$), the CPU time on a modern desktop computer is less than 3 min. Of course, the CPU time increases with the model dimensions. The other major advantage is that the outputs are generated in multiple formats (corner-point-geometry format, GEOEAS/GSLIB format) and can easily be used in modeling, visualization, and fluid-flow-simulation packages. Well and seismic data conditioning are being developed. The combination of the corner-point-geometry format and the modeled depositional surfaces facilitates horizon modeling and thus separate horizon modeling is not required.

7. Limitations

A number of geomorphic parameters and concepts, other than those stated in this paper, could be incorporated in the modeling process. These include erodability index (Table 1), Strahler's network ordering (relates stream ordering in terms of network architecture, Strahler, 1952), Horton's laws (regarding distributions of stream lengths, Horton, 1945), Hack's law (relates basin length to basin area, Hack, 1957) and others. The simulation of deepwater-reservoir elements, particularly lobe forms, could be improved by incorporating quantitative aspects and information based on concepts appropriate to deepwater-depositional systems and similar to the above-mentioned laws or concepts. Additional observations from flume studies, geological process experiments, outcrop, and stratigraphic studies will augment future modeling attempts.

Methods are being investigated to condition the deepwater-reservoir models to well and seismic data. Other modifications to incorporate deepwater-reservoir architectural elements such as levees

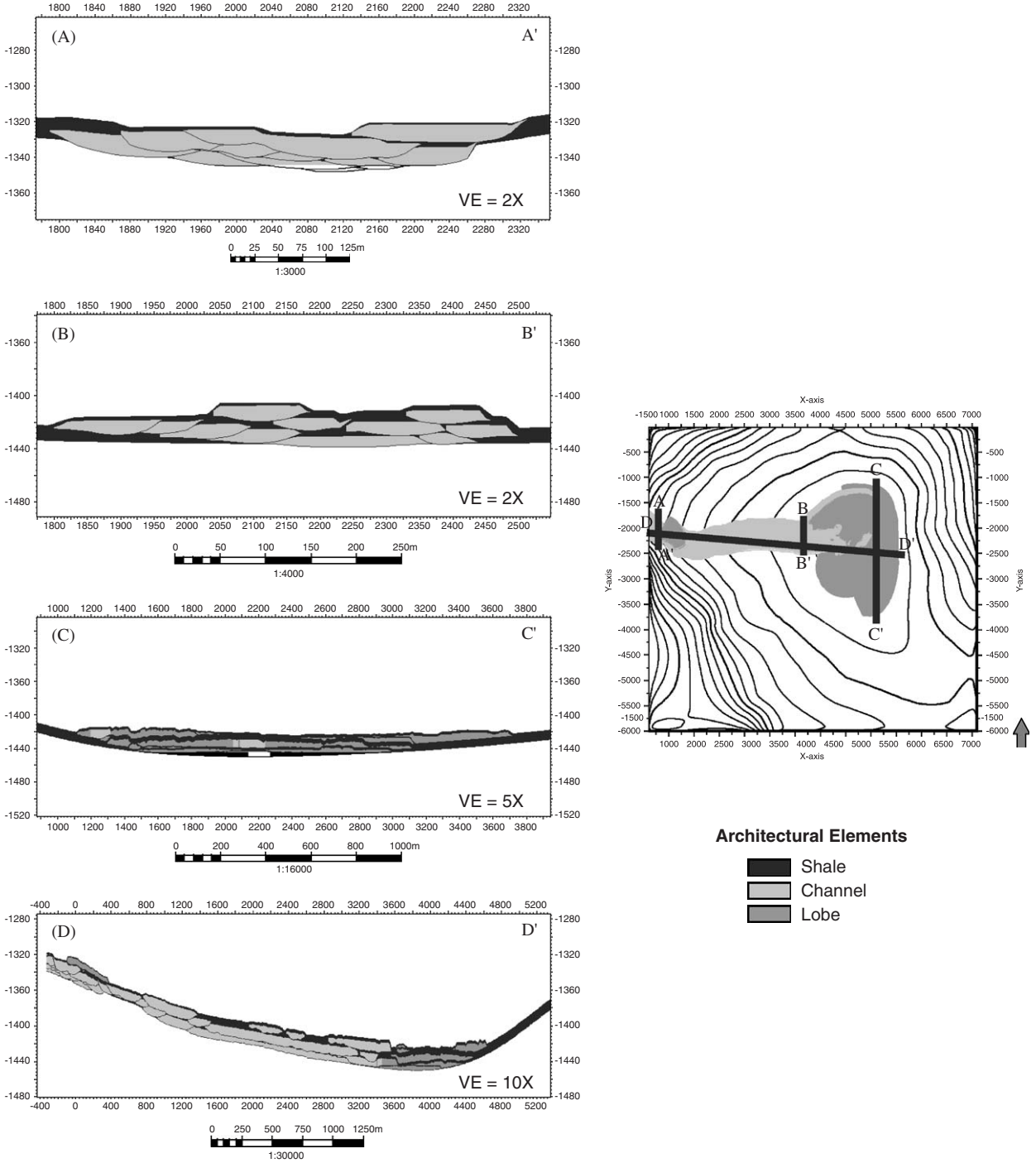

Fig. 9. Cross-sections that illustrate reservoir architecture of channel-lobe and condensed-section events of simple example. Cross-sections highlight stacking patterns and architecture for proximal, intermediate, and distal locations and longitudinal to primary direction of deposition. Proximal cross-section, AA′, shows compensational channel stacking and erosion surfaces. Intermediate cross-section, BB′, reveals a lower degree of erosion/scour and lower net-to-gross ratio compared to section A–A′. Distal cross-section, CC′, shows sheet-form nature of reservoir architecture. A longitudinal cross-section, DD′, illustrates continuity of reservoir architecture. VE = vertical exaggeration.

(channel-levee deposits) and sub-facies within depositional settings will also be explored in future versions. We also recognize the limitation of the developed approach that it overlooks the role of concurrent-structural deformation in sediment accommodation and bathymetry. Future investigation could possibly address these important phenomena within the modeling process.

8. Concluding remarks

ModDRE is a deepwater-reservoir modeling approach to construct realistic 3D-reservoir architectures and models. This computationally efficient modeling technique will lend itself for use in large-scale real-time reservoir modeling and inversion problems. ModDRE incorporates both stratigraphic and geomorphic constraints. This modeling approach retains the flexibility of the stochastic approaches as well as the essence of geological process-based modeling approaches.

ModDRE attempts to mimic the conceptual depositional and erosional processes in deepwater settings unlike some purely stochastic approaches. Through this modeling approach, it is possible to quantify the tortuosity, curvature, gradients, bathymetric changes, and a number of other parameters for channel bodies and corroborate those with our expert knowledge. The approach is computationally efficient. The other major advantage is that the outputs are generated in multiple formats and can easily be used in modeling, visualization, and fluid-flow-simulation packages.

Acknowledgements

This research is funded through a grant from the American Chemical Society, Petroleum Research Fund and through the Energy and Minerals Applied Research Center at the University of Colorado at Boulder. We thank Thomas A. Jones and Lynn Watney for their useful reviews of this manuscript. We also thank the editor of Computers & Geosciences, Graeme F. Bonham-Carter, for his suggestions on revision of the manuscript.

References

Beaubouef, R.T., Rossen, C., Zelt, F.B., Sullivan, M.D., Mohrig, D.C., Jennette, D., 1999. Deepwater Sandstones, Brushy Canyon Formation, West Texas: Field Guide. In: American Association of Petroleum Geologists (AAPG) Hedberg Field Research Conference, Continuing Education Course Note Series #40, 44pp.

Beaubouef, R.T., Abreu, V., Van Wagoner, J.C., 2003. Basin 4 of the Brazos–Trinity slope system, western Gulf of Mexico: the terminal portion of a late Pliestocene lowstand systems tract. In: Roberts, H.H., Rosen, N.C., Fillon, R.H., Anderson, J.B. (Eds.), Gulf Coast Section—Society of Sedimentary Geology (GCSSEPM) Foundation 23rd Annual Bob F. Perkins Research Conference, pp. 182–203.

Clark, J.D., Pickering, K.T., 1996. Submarine Channels: Processes and Architecture. Vallis Press, London 231pp.

Deutsch, C.V., Journel, A., 1998. GSLIB: Geostatistical Software Library and User's Guide, 2nd ed. Oxford University Press, New York 369pp.

Deutsch, C.V., Tran, T.T., 2002. FLUVSIM: a program for object-based stochastic modeling of fluvial depositional systems. Computers & Geosciences 28 (4), 525–535.

GeoQuest, 2004. ECLIPSE Reference Manual. Schlumberger, Houston, TX 2092pp.

Hack, J.T., 1957. Studies of longitudinal stream profiles in Virginia and Maryland. US Geological Survey Professional Paper 294-B, pp. 45–97.

Haldorsen, H.H., Chang, D.W., 1986. Notes on stochastic shales, from outcrop to simulation model. In: Lake, L.W., Carroll, H.B. (Eds.), Reservoir Characterization. Academic Press, London, pp. 445–485.

Haldorsen, H.H., Lake, L.W., 1984. A new approach to shale management in field-scale model. Society of Petroleum Engineers Journal April, 447–457.

Horton, R.E., 1945. Erosional development of streams and their drainage basins; hydrophysical approach to quantitative morphology. Bulletin of the Geological Society of America 56 (3), 275–370.

Johnson, S.D., Flint, S., Hinds, D., DeVille Wickens, H., 2001. Anatomy, geometry and sequence stratigraphy of basin floor to slope turbidite systems, Tanqua Karoo, South Africa. Sedimentology 48, 97–1023.

Jones, T.A., 2001. Using flowpaths and vector fields in object-based modeling. Computers & Geosciences 27 (2), 133–138.

Martinez, P.A., Harbaugh, J.W., 1993. Simulating Near-shore Environments. Pergamon Press, Oxford 265pp.

Mutti, E., Normark, W.R., 1991. An integrated approach to the study of turbidite systems. In: Weimer, P., Link, M.H. (Eds.), Seismic Facies and Sedimentary Processes of Submarine Fans and Turbidite Systems. Springer, New York, pp. 75–106.

Pyrcz, M.J., Catuneanu, O., Deutsch, C.V., 2005. Stochastic surface-based modeling of turbidite lobes. American Association of Petroleum Geologists Bulletin 89 (2), 177–191.

Strahler, A.N., 1952. Hypsometric (area–altitude) analysis of erosional topography. Geological Society of America Bulletin 63, 1117–1142.

Strebelle, S., Payrazyan, K., Caers, J., 2002. Modeling of a deepwater turbidite reservoir conditional to seismic data using multiple-point geostatistics. In: Society of Petroleum Engineers (SPE) Annual Conference and Technical Meeting, SPE 77429, San Antonio, Texas, 16pp.

Tarboton, D.G., 1997. A new method for the determination of flow directions and contributing areas in grid digital elevation models. Water Resources Research 33 (2), 309–319.

Tarboton, D.G., 2003. Terrain analysis using digital elevation models in hydrology. In: 23rd Environmental Systems

Research Institute (ESRI) International Users Conference, San Diego, CA, 13pp.

Tetzlaff, D.A., Harbaugh, J.W., 1989. Simulating Clastic Sedimentation. van Nostrand Reinhold, New York 202pp.

Weimer, P., Slatt, R.M., 2004. Petroleum Systems of Deepwater Settings. 2004 Distinguished Instructor Short Course. Society of Exploration Geophysicists, European Association of Geoscientists and Engineers, Tulsa, OK 470pp.

Xie, Y., Deutsch, C.V, Cullick, S., 2000. Surface geometry and trend modeling for integration of stratigraphic data in reservoir models. In: Kleingeld, W.J., Krige, D.G., (Eds.), Geostats 2000, vol. 1, Cape Town, pp. 287–295.